JOC Article

Sequential *O*- and *N*-Acylation Protocol for High-Yield Preparation and Modification of Rotaxanes: Synthesis, Functionalization, Structure, and Intercomponent Interaction of Rotaxanes

Yuya Tachibana, Hiroaki Kawasaki, Nobuhiro Kihara,*,† and Toshikazu Takata*,‡

Department of Applied Chemistry, Graduate School of Engineering, Osaka Prefecture University, Sakai, Osaka 599-8531, Japan

ttakata@polymer.titech.ac.jp

Received January 24, 2006

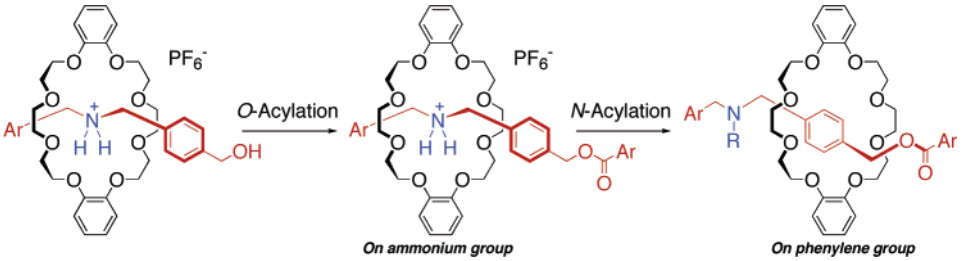

A pseudorotaxane consisting of a 24-membered crown ether and secondary ammonium salt with the hydroxy group at the terminus was quantitatively acylated by bulky acid anhydride in the presence of tributylphosphane as catalyst to afford the corresponding rotaxane in high yield. Large-scale synthesis without chromatographic separation was easily achieved. The ammonium group in the resulting rotaxane was quantitatively acylated with excess electrophile in the presence of excess trialkylamine. Various *N*-functionalized rotaxanes were prepared by this sequential double-acylation protocol. ^{1}H NMR spectra and X-ray crystallographic analyses of the rotaxanes showed that the crown ether component was captured on the ammonium group in ammonium-type rotaxane by strong hydrogen-bonding intercomponent interaction. The conformation around the ammonium group was fixed by the hydrogen-bonding interaction. Meanwhile, the conformation of the amide-type rotaxane was determined by the weak CH/π interaction between the methylene group in crown ether and the benzene ring of the axle component. The *N*-acylation of ammonium-type rotaxane is useful for the preparation of both functionalized rotaxanes and weak intercomponent interaction-based rotaxanes.

Introduction

Rotaxane and catenane are characterized by the mechanical bonding of their components.[1] In directed syntheses of rotaxane,[2] the components that make up rotaxane are preorganized by some intermolecular interaction before the interlocked structure is fixed. The intermolecular interaction becomes the intercomponent interaction via the preparation procedure. Therefore, it is obvious that the intercomponent interaction determines the features of the mechanical bonding.

A variety of applications have been projected for rotaxanes on the basis of mechanical bonding. Molecular devices are among the most promising applications of rotaxane,[3] e.g., a molecular memory in which the position of the wheel component on the axle component provides one bit of information and a molecular machine in which a labile mechanical bonding works as a nanosized gear or piston. To achieve a successful

† Present address: Department of Chemistry, Faculty of Science, Kanagawa University, 2946 Tsuchiya, Hiratsuka 259-1293, Japan. Tel: +81-463-59-4111. Fax: +81-463-58-9684. E-mail: kihara@kanagawa-u.ac.jp.

‡ Present address: Department of Organic and Polymeric Materials, Tokyo Institute of Technology, Ookayama, Meguro, Tokyo 152-8552, Japan. Tel: +81-3-5734-2898. Fax: +81-3-5734-2888.

(1) (a) Shill, G. *Catenanes, Rotaxanes, and Knots*; Academic Press: New York, 1971. (b) Sauvage, J.-P., Dietrich-Buchecker, C., Eds. *Molecular Catenanes, Rotaxanes, and Knots*; Wiley-VCH: Weinheim, 1999. (c) Walba, D. M. *Tetrahedron* **1985**, *41*, 3161−3212. (d) Breault, G. A.; Hunter, A.; Mayers, P. C. *Tetrahedron* **1999**, *55*, 5265−5293.

(2) (a) Dietrich-Buchecker, C.; Sauvage, J.-P. *Chem. Rev.* **1987**, *87*, 795−810. (b) Sauvage, J.-P. *Acc. Chem. Res.* **1990**, *23*, 319−327. (c) Amabilino, D. B.; Stoddart, *J. F. Chem. Rev.* **1995**, *95*, 2725−2828. (d) Vöglte, G.; Dünnwald, T.; Schmidt, T. *Acc. Chem. Res.* **1996**, *29*, 451−460. (e) Fyfe, M. C. T.; Stoddart, J. F. *Adv. Supramol. Chem.* **1999**, 1−53. (f) Hubin, T. J.; Busch, D. H. *Coord. Chem. Rev.* **2000**, *200−202*, 5−52. (g) Takata, T.; Kihara, N. *Rev. Heteroatom Chem.* **2000**, *22*, 197−218.

10.1021/jo0601563 CCC: $33.50
Published on Web 06/06/2006

application for rotaxanes, it is necessary to control the relative conformation between the wheel and the axle components. This can be attained by controlling the intercomponent interaction. Sauvage et al. first demonstrated the conformation control of an interlocked compound based on metal−ligand interaction.[4] By elimination of the metal ion carrying the intercomponent interaction, a certain conformation change was successfully induced. Further, the redox reaction-induced change of coordination numbers of copper ion was also used for conformation control.[5] Stoddart et al. prepared various interlocked compounds based on charge-transfer interaction or hydrogen-bonding interaction of ammonium salt and crown ether and demonstrated that intercomponent conformation could be precisely controlled by deprotonation or redox reaction of the ammonium group via control of the intercomponent charge-transfer interaction.[6] Further, Nakashima et al. reported rotaxanes based on the hydrophobic interaction between the *trans*-azobenzene group and cyclodextrin and showed that intercomponent conformation could be controlled by photoinduced isomerization of the azobenzene group to the cis form.[7] Leigh et al. reported rotaxanes based on the hydrogen-bonding interaction between fumaramide and macrolactam with secondary amide moieties and demonstrated that the photoinduced isomerization of fumaramide to maleamide caused a change in intercomponent conformation.[8] In these systems, conformation control was attained by some external stimuli that removed the intercomponent interaction preintroduced in the preparation step. Since the intercomponent interaction in interlocked systems is inseparable from the combination of components used for the construction of the system, there are scant choices of methods to control the conformation. If intercomponent interaction is independent of the combination of components, not only weak and labile interaction but also a combination of different types of interactions can be used to control conformation. Therefore, the development of a general method to introduce desired functional groups into the rotaxane after the elimination of intercomponent interaction preintroduced is highly desirable. Such a method, if developed, can make a variety of functionalized rotaxanes possible.

CHART 1

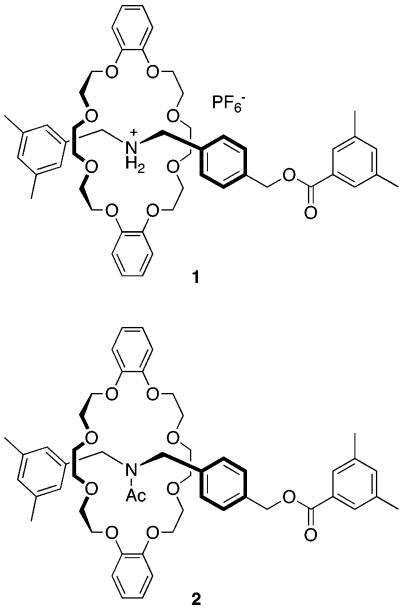

We previously reported one of the most efficient methods to synthesize rotaxanes consisting of crown ethers and secondary ammonium salts (Chart 1).[9] A pseudorotaxane possessing a hydroxy group at the axle terminus was quantitatively acylated by bulky acid anhydride in the presence of tributylphosphane as catalyst[10] to afford the corresponding rotaxane in up to 90% yield. In the resulting rotaxane, the intercomponent interaction between the ammonium group and crown ether was so strong that the acidity of the secondary ammonium group was unusually low.[11] The *N*-acylation of the ammonium group proceeded slowly in the presence of excess triethylamine to give the corresponding *N*-acylated rotaxanes quantitatively (Chart 1). By *N*-acylation, the intercomponent interaction was expected to be eliminated. However, the intercomponent interaction working in the resulting rotaxane was unclear.

This sequential double-acylation protocol has made practical access to functionalized rotaxanes easy. Since both crown ether and secondary ammonium salt are well-studied artificial com-

(3) (a) Balzani, V.; Credi, A.; Raymo, F. M.; Stoddart, J. F. *Angew. Chem., Int. Ed*. **2000**, *39*, 3348−3391. (b) Pease, A. R.; Jeppesen, J. O.; Stoddart, J. F.; Luo, Y.; Collier, C. P.; Heath, J. R. *Acc. Chem. Res*. **2001**, *34*, 433−444. (c) Ballardini, R.; Balzani, V.; Credi, A.; Gandolfi, M. T.; Venturi, M. *Acc. Chem. Res.* **2001**, *34*, 445−455. (d) Harada, A. *Acc. Chem. Res*. **2001**, *34*, 456−464. (e) Schalley, C. A.; Beizai, K.; Vögtle, F. *Acc. Chem. Res*. **2001**, *34*, 465−476. (f) Collin, J.-P.; Dietrich-Buchecker, C.; Gaviña, P.; Jimenez-Molero, M. C.; Sauvage, J.-P. *Acc. Chem. Res*. **2001**, *34*, 465−476. (g) Collin, J.-P.; Sauvage, J.-P. *Chem. Lett.* **2005**, *36*, 742−747. (h) Sauvage, J.-P. *Chem. Commun.* **2005,** *12*, 1507−1510. (i) Badji, J. D.; Nelson, A.; Cantrill, S. J.; Turnbull, W. B.; Stoddart, J. F. *Acc. Chem. Res.* **2005**, *38*, 723−732.

(4) Dietrich-Buchecker, C.; Sauvage, J.-P.; Kern, J. M. *J. Am. Chem. Soc*. **1984**, *106*, 3043−3045

(5) (a) Collin, J.-P.; Gaviña. P.; Sauvage, J.-P. *New J. Chem*. **1997**, *21*, 525−528. (b) Armaroli, N.; Balzani, V.; Collin. J.-P.; Gaviña. P.; Sauvage, J.-P.; Ventura, B. *J. Am. Chem. Soc*. **1999**, *121*, 497−4408. (c) Collin, J.-P.; Dietrich-Buchecker, C.; Gavina, P.; Jimenez-Molero, M.-C.; Sauvage, J.-P. *Acc. Chem. Res.* **2001**, *34*, 477.

(6) (a) Bissell, R. A.; Córdova, E.; Kaifer, A. E.; Stoddart, J. F. *Nature* **1994**, *369*, 133−137. (b) Amabilino, D. B.; Ashton, D. R.; Boyd, S. E.; Cómez-López, M.; Hayes, W.; Stoddart, J. F. *J. Org. Chem*. **1997**, *62*, 3062−3075. (c) Ashton, P. E.; Ballardini, R.; Balzani, V.; Baxter, I.; Credi, A.; Fyfe, M. C. T.; Gandolfi, M. T.; Cómez-López, M.; Martínez-Díaz, M.-V.; Piersanti, A.; Spencer, N.; Stoddart, J. F.; Venturi, M.; White, A. J. P.; Williams, D. J. *J. Am. Chem. Soc*. **1998**, *120*, 11932−11942. (d) Jeppesen, J. O.; Perkins, J.; Becher, J.; Stoddart, J. F. *Angew. Chem., Int. Ed*. **2001**, *40*, 1216−1221. (e) Garaudee, S.; Silvi, S.; Venturi, M.; Credi, A.; Flood, AH.; Stoddart, J. F. *ChemPhysChem* **2005**, *6*, 2145. (f) Elizarov, A. M.; Chiu, S. H.; Stoddart, J. F. *J. Org. Chem.* **2002**, *67*, 9175.

(7) (a) Kunitake, M.; Kotoo, K.; Manabe, O.; Muramatsu, T.; Nakashima, N. *Chem. Lett*. **1993**, *21*, 1033−1036. (b) Murakami, H.; Kawabuchi, A.; Kotoo, K.; Kunitake, M.; Nakashima, N. *J. Am. Chem. Soc.* **1997**, *119*, 7605−7606. (c) Murakami, H.; Kawabuchi, A.; Matsumoto, R.; Ido, T.; Nakashima, N. *J. Am. Chem. Soc.* **2005**, *127*, 15891−15899.

(8) (a) Brouwer, A. M.; Frochot, C.; Gatti, F. G.; Leigh, D. A.; Mottier, L.; Paolucci, F.; Roffia, S.; Wurpel, G. W. H. *Science* **2001**, *292*, 2124−2128. (b) Wurpel, G. W. H.; Brouwer, A. M.; van Stokkum, I. H. M.; Farran, A.; Leigh, D. A. *J. Am. Chem. Soc*. **2002**, *123*, 11327−11328. (c) Pérez, E. M.; Dryden, D. T. F.; Leigh, D. A.; Teobaldi, G.; Zerbetto, F.: *J. Am. Chem. Soc*, **2004**, *126*, 12210−12211. (d) Chatterjee, M. N.; Kay, E. R.; Leigh, D. A. *J. Am. Chem. Soc.* **2006**, *128*, 4058. (e) Kay, E. R.; Leigh, D. A. *Top. Curr. Chem.* **2005**, *262*, 133.

(9) (a) Kawasaki, H.; Kihara, N.; Takata, T. *Chem. Lett.* **1999**, *28*, 1015−1016. (b) Kihara, N.; Shin, J.-I.; Ohga, Y.; Takata, T. *Chem. Lett*. **2001**, *30*, 592−593. (c) Kihara, N.; Nakakoji, N.; Takata, T. *Chem. Lett*. **2002**, *31*, 924−925. (d) Furusho, Y.; Oku.; Hasegawa, T.; Tsuboi, A.; Kihara, N.; Takata, T. *Chem. Eur. J*. **2003**, *9*, 2895−2903. (e) Furusho, Y.; Rajkumar, G. A.; Oku, T.; Takata, T. *Tetrahedron* **2002**, *58*, 6609−6613. (f) Furusho, Y.; Sasabe, H.; Natsui, D.; Murakawa K−i.; Harasa, T.; Takata, T. *Bull. Chem. Soc. Jpn*. **2004**, *77*, 179−185. (g) Sasabe, H.; Kihara, N.; Mizuno, K.; Ogawa, A.; Takata, T. *Tetrahedron Lett.* **2005**, *46*, 3851−3853.

(10) Vedejs, E. V.; Diver, S. T. *J. Am. Chem. Soc*. **1993**, *115*, 3358−3359.

(11) Kihara, N.; Tachibana, Y.; Kawasaki, H.; Takata, T. *Chem. Lett*. **2000**, *29*, 506−507.

pounds, these compounds present few structural limitations.[2e−g,12] Various functionalized crown ethers are available,[9f,12f,j] and the large-scale synthesis of crown ether is also possible. Since acylation is one of the most commonly studied reactions, many acylation reagents and techniques can be used. Further, the elimination of intercomponent interaction preintroduced and the introduction of new functional groups can be simultaneously attained in the *N*-acylation process. As a result, the combination of crown ether and secondary ammonium salt along with the sequential double-acylation protocol seems to provide one of the most suitable systems to obtain rotaxanes with the desired functionalities (Chart 2).

To establish the sequential acylation protocol as a sophisticated method to functionalize rotaxanes, we have studied the conformations of rotaxanes before and after *N*-acylation. Although it was assumed that little intercomponent interaction would remain in the rotaxane after *N*-acylation, some weak interactions were actually operative instead of strong hydrogen-bonding interaction preintroduced. Since weaker interactions are easier to control than stronger ones, the rotaxane becomes more environment-sensitive via *N*-acylation. This feature may be useful for the construction of sensitive molecular devices. In this paper, we wish to report the high-yield synthesis, functionalization, structures, and intercomponent interaction of rotaxanes obtained by the sequential double acylation protocol. The details of the sequential acylation protocol are also discussed.

Synthesis of Rotaxane by *O*-Acylation. Dibenzylammonium salt **3** bearing 3,5-dimethylphenyl and hydroxy groups at each terminus was used as the axle component. While **3** is only slightly soluble in less polar organic solvents, it dissolved in dichloromethane or chloroform by the addition of 1 equiv of dibenzo-24-crown-8 (DB24C8). This phenomenon indicates the formation of a stable complex **3**−DB24C8.

The successful synthesis of [2]rotaxane **1** by *O*-acylation with 3,5-dimethylbenzoic anhydride **4a** clearly proved that the complex has a pseudorotaxane structure (Scheme 1). The dichloromethane solution of a mixture of **3** and DB24C8 was treated with **4a** in the presence of tributylphosphane as catalyst[9a] to afford **1** in 90% yield after purification by preparative gel permeation chromatography. The rotaxane structure of **1** was demonstrated by ^{1}H NMR, FAB-MS, and IR spectra. Finally,

CHART 2

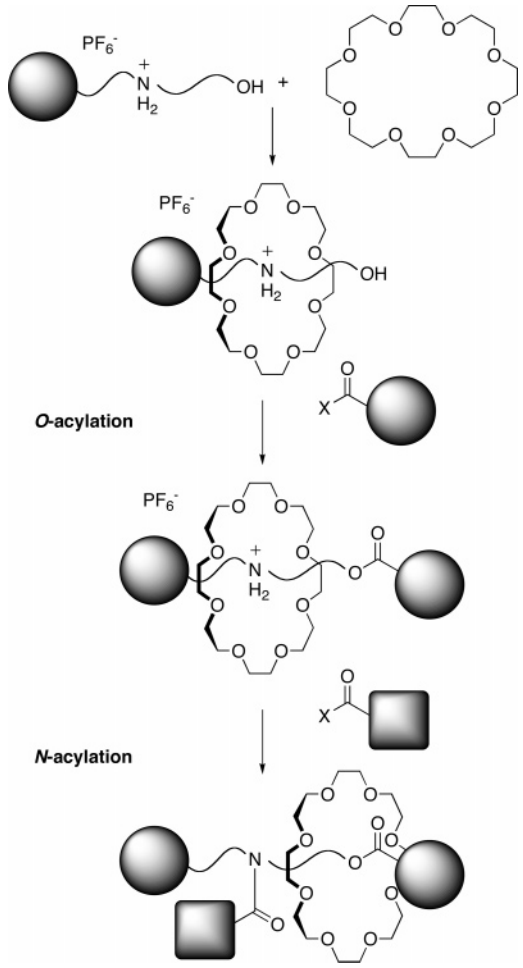

X-ray crystallographic analysis of **1** confirmed the rotaxane structure (vide infra).

The results of the *O*-acylative end-capping reactions of **3** are summarized in Table 1. The reaction did not proceed without catalyst (run 1). Tributylphosphane was a very effective catalyst when used with acid anhydride (run 2). Since phosphane is only weakly basic, it did not prevent hydrogen bonding between the ammonium salt and crown ether moieties. Interestingly, acid chloride **4b**, which is a generally more active acylation reagent than acid anhydride, did not work as an effective end-capping

SCHEME 1

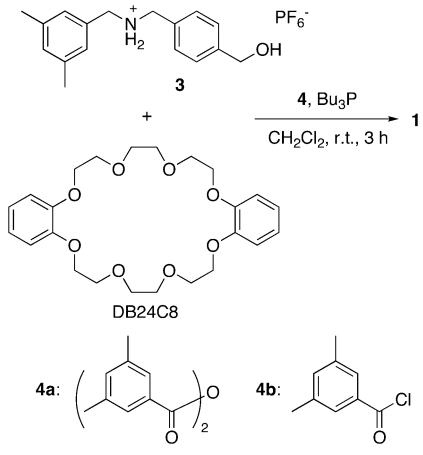

(12) (a) Kolchinski, A. G.; Busch, D. H.; Alcock, N. W. *J. Chem. Soc., Chem. Commun.* **1995**, 1289−1291. (b) Ashton, P. R.; Campbell, P. J.; Chrystal, E. J. T.; Glink, P. T.; Menzer, S.; Philp, D.; Spencer, N.; Stoddart, J. F.; Tasker, P. A.; Williams, D. J. *Angew. Chem., Int. Ed. Engl.* **1995**, *34*, 1865−1869. (c) Ashton, P. R.; Glink, P. T.; Stoddart, J. F.; Taasker, P. A.; White, A. J. P.; Williams, D. J. *Chem. Eur. J.* **1996**, *2*, 729−736. (d) Ashton, P. R.; Baxter, I.; Fyfe, M. C. T.; Raymo, F. M.; Spencer, N.; Stoddart, J. F.; White, A. J. P.; Williams, D. J. *J. Am. Chem. Soc.* **1998**, *120*, 2297−2307. (e) Yamaguchi, N.; Gibson, H. W. *Angew. Chem., Int. Ed. Engl.* **1999**, *38*, 143−147. (f) Cantrill, S. J.; Fulton, D. A.; Heiss, A. M.; Pease, A. R.; Stoddart, J. F.; White, A. J. P.; Williams, D. *J. Chem. Eur. J.* **2000**, *6*, 2274−2287. (g) Matthew, J. C.; Fyfe, M. C. T.; Stoddart, J. F. *J. Org. Chem.* **2000**, *65*, 1937−1946. (h) Glink, P. T.; Oliva, A. I.; Stoddart, J. F.; White, A. J. P.; Williams, D. J. *Angew. Chem., Int. Ed.* **2001**, *40*, 1870−1875. (i) Zehnder, D. W.; Smithrud, D. B. *Org. Lett.* **2001**, *3*, 2485−2487. (j) Chiu, S.-H.; Rowan, S. J.; Cantrill, S. J.; Stoddart, J. F.; White, A. J. P.; Williams, D. J. *Chem. Eur. J.* **2002**, *8*, 5170−5183. (k) Asakawa, M.; Ikeda, T.; Yui, N.; Shimizu, T. *Chem. Lett.* **2002**, *31*, 174−175. (l) Tokunaga, Y.; Kakuchi, S.; Akasaka, K.; Nishikawa, N.; Shimomura, Y.; Isa, K.; Seo, T. *Chem. Lett.* **2002**, *31*, 810−811. (m) Ikeda, T.; Asakawa, M.; Goto, M.; Nagawa, Y.; Shimizu, T. *Eur. J. Org. Chem.* **2003**, 3744−3751. (n) Tokunaga, Y.; Kakuchi, S.; Akasaka, K.; Hisada, K.; Shimomura, Y.; Suzuka, K. *Chem. Commun.* **2003**, 2250−2251. (o) Arico, F.; Chang, T.; Cantrill, S. J.; Khan, S. I.; Stoddart, J. F. *Chem. Eur. J.* **2005**, *11*, 4655−4666.

TABLE 1. Effect of Reaction Conditions on the Preparation of 1[a]

run	catalyst (mol %)	additive[b]	[DB24C8] [**3**]	solvent	acylation reagent	yield[c]/ %
1	none	none	3.00	CH_2Cl_2	**4a**	0
2	Bu_3P (10)	none	3.00	CH_2Cl_2	**4a**	90
3	Bu_3P (10)	none	3.00	CH_2Cl_2	**4b**	10
4	Bu_3P (10)	$AgPF_6$	3.00	CH_2Cl_2	**4b**	29
5	Bu_3P (1000)	$AgPF_6$	3.00	CH_2Cl_2	**4b**	50
6	DMAP (10)	none	3.00	CH_2Cl_2	**4a**	3
7	DMAP (50)	Et_3N	3.00	CH_2Cl_2	**4a**	13
8	DMAP (50)	Et_3N	3.00	CH_2Cl_2	**4b**	7
9	Bu_3P (10)	none	3.00	benzene[d]	**4a**	88
10	Bu_3P (10)	none	3.00	dioxane[d]	**4a**	74
11	Bu_3P (10)	none	3.00	acetonitrile[d]	**4a**	90
12	Bu_3P (10)	none	1.05	CH_2Cl_2	**4a**	89

[a] Reactions were carried out at room temperature for 3 h. [**3**] = 0.5 mol/L. [b] 1.5 equiv was used. [c] Isolated yield. [d] Heterogeneous system.

agent (run 3). The hydrogen-bonding interaction of chloride ion with ammonium salt is supposed to have prevented the complexation of the ammonium salt with the crown ether. To remove the chloride ion from the system, the addition of silver salt was investigated.[9b] When 1.5 equiv of silver hexafluorophosphate was added, the yield of **1** improved only slightly (run 4). It was anticipated that the concentration of tributylphosphane, the catalyst of acylation, would decrease due to the coordination to silver ion. When the reaction was carried out in the presence of an excess amount of tributylphosphane, the yield of **1** increased up to 50% (run 5). When 4-(dimethylamino)pyridine (DMAP) was used as catalyst instead of tributylphosphane, only 3% of **1** was obtained (run 6), indicating the effectiveness of phosphane as catalyst. The addition of triethylamine to the DMAP-catalyzed system as base enhanced the yield of **1** only a little (runs 7 and 8). Since triethylamine deprotonated **3** to destroy the **3**−DB24C8 complex, the enhancement of the acylation reaction did not result in an increase of the yield of **1**. When benzene, dioxane, or acetonitrile was used as solvent, **1** was obtained in high yields although the system was heterogeneous in these solvents (runs 9−11). Since the **3**−DB24C8 complex is more soluble in organic solvent than **3** itself, it was acylated preferentially to give **1** in excellent yield. Although the hydrogen-bonding interaction should be weakened in polar solvents such as dioxane and acetonitrile, no considerable decrease in the yield of **1** was observed. Further, the excess amount of DB24C8 was unnecessary (run 12). It was concluded that the superior catalytic activity and low basicity of tributylphosphane ensures the high-yield synthesis of **1**.

The large-scale synthesis of **1** was quite easily accomplished. Thus, starting from 4.49 g (10.0 mmol) of DB24C8 and 3.61 g (9.00 mmol) of **3**, 6.91 g (7.04 mmol) of pure **1** (78%) was simply obtained after recrystallization from ethyl acetate. Only 10 mL of solvent (dichloromethane) was necessary for the synthesis because the ratio pseudorotaxane/**3** increased at higher concentration conditions. Since no chromatographic purification was necessary in the course of the preparation of **3**, **1** was totally prepared from commercially available chemicals without column chromatography.

Successful syntheses of various [2]rotaxanes confirmed the generality and versatility of the tributylphosphane-catalyzed *O*-acylative end-capping method as summarized in Table 2. The

TABLE 2. Preparation of Various [2]Rotaxanes via the Tributylphosphine-Catalyzed *O*-Acylation[a]

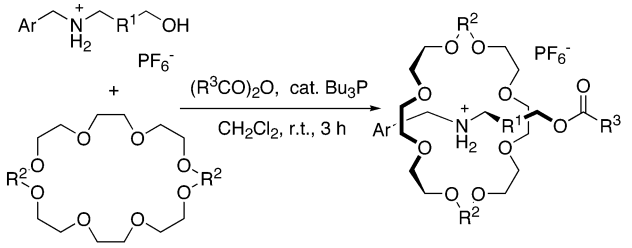

Ar	R^1	R^2	R^3	rotaxane	yield/%[b]
2,6-dimethylphenyl			2,6-dimethylphenyl	**1**	90
2,6-dimethylphenyl	$-CH_2-$		2,6-dimethylphenyl	**5**	78
2,6-dimethylphenyl			2,6-dimethylphenyl	**6**	88
9-anthryl	$-CH_2-$		2,6-dimethylphenyl	**7**	82
2,6-dimethylphenyl			2,4,6-trimethylphenyl	**8**	85[c]

[a] Reactions were carried out at room temperature in CH_2Cl_2 (0.5 mol/L) for 3 h in the presence of 3 equiv of crown ether and 10 mol % of Bu_3P. [b] Isolated yield. [c] Reaction was carried out for 24 h.

SCHEME 2

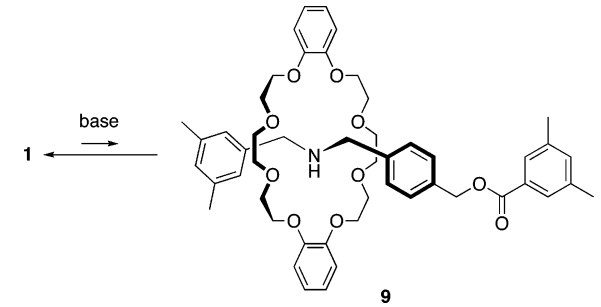

9

structures of all products were determined by elemental analyses in addition to spectral characterization. Dicyclohexano-24-crown-8 could be used as a wheel without a decrease in yield to afford [2]rotaxane **6**. The results revealed that the $\pi-\pi$ interaction between the axle and the wheel is not important in this case.[13] Although the end-capping with bulky pivalic anhydride was slow, [2]rotaxane **8** was obtained in high yield (85%) after a prolonged reaction period. Thus, the present synthetic method of [2]rotaxanes tolerates a wide range of solvents and components.

***N*-Acylative Neutralization.** Because of the strong intramolecular hydrogen-bonding interaction, attempts to neutralize **1** by bases such as sodium carbonate and calcium hydride were

(13) Stoddart et al. mentioned the importance of $\pi-\pi$ interaction between the axle and the wheel: Ashton, P. R.; Glink, P. T.; Stoddart, J. F.; Menzer, S.; Tasker, P. A.; White, A. J. P.; Williams, D. J. *Tetrahedron Lett.* **1996**, *2*, 6217−6220.

SCHEME 3

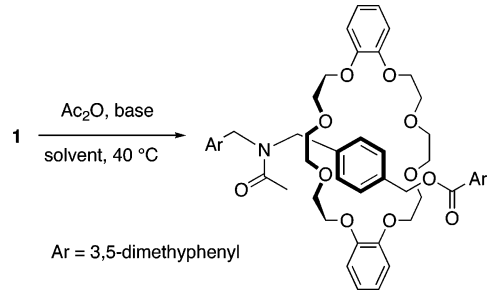

unsuccessful, as indicated in a previous report (Scheme 2).[11] Although the kinetic acidity of **1** is smaller than ethanol, pyrrole, or general ammonium salt,[11,12j] free amine−rotaxane **9** may actually still be present in the equilibrium when **1** is treated with a base. The presence of **9** was successfully proven by trapping **9** with suitable electrophiles.

The reaction of **1** with 2 equiv of triethylamine and 2 equiv of acetic anhydride in acetonitrile-d_3 was monitored by ^{1}H NMR. Despite the simple amide formation reaction, the reaction proceeded extremely sluggishly: 48% of **1** was consumed after 2 weeks. From the reaction mixture, *N*-acetylated [2]rotaxane **2** was isolated in 48% yield. No other product was observed. Although the selectivity of the reaction was high, as in general amide formation reaction, the reaction rate was slow due to the low concentration of **9** probably resulting from the strong intercomponent hydrogen-bonding interaction. It should be noted that amide **2** showed a smaller R_f value (R_f 0.22) than ammonium salt **1** (R_f 0.54) on silica gel TLC (eluent: CH_2Cl_2−CH_3CN 10/1 v/v), indicating that **2** is more polar than **1**. The interaction of silica gel with **1** is weaker than that with **2** because the ammonium group is surrounded by crown ether in **1**.

To increase the concentration of **9** in the system, a 20 equimolar amount of triethylamine was used, and 100% of **2** was isolated after 8 d reaction. Further, when the reaction was carried out in acetonitrile in the presence of a 5 equimolar amount of triethylamine and 10 equiv of acetic anhydride at 40 °C for 24 h, **2** was obtained in 100% yield. These results indicate that both a long reaction period and an excess amine and electrophile are necessary for quantitative *N*-acylation. Thus, the effects of solvent, base, and their concentrations were examined (Scheme 3). A reaction was carried out using 5 equiv of tertiary amine and 2 equiv of acetic anhydride as the electrophile at 40 °C for 24 h to evaluate the effects of reaction conditions. Results are summarized in Table 3.

There was a large solvent effect on the yield of **2** (runs 1, 3−8). In more polar solvents such as acetonitrile or DMF, the reaction proceeded more rapidly.

Since only 60% of **2** was obtained in pyridine, which is one of the most basic and polar solvents (run 6), the effect of tertiary amines was studied (runs 1 and 9−17). The result is confusing. While amines bearing sp^3-hybridized nitrogen such as triethylamine and ethyldiisopropylamine (DIPEA) worked effectively, amines bearing sp^2-hybridized nitrogen such as pyridine, DBU, and imidazole showed little activity. When the reaction was carried out in pyridine in the absence of triethylamine, the yield was only 6% (run 14). It should be noted that the most basic amine, DBU, was ineffective, while the most bulky amine, DIPEA, was effective as well as triethylamine. Therefore, thermodynamic basicity is unrelated to the activity of amines, and the kinetics of proton abstraction from the ammonium group

TABLE 3. Effect of Solvent and Base in the *N*-Acylation of 1[a]

run	solvent	base (equiv)	time/h	yield/%
1	acetonitrile	Et_3N (5)	24	82
2	acetonitrile	Et_3N (20)	192	100
3	acetonitrile	Et_3N (5)	24	100[b]
4	THF	Et_3N (5)	24	39
5	$CHCl_3$	Et_3N (5)	24	48
6	pyridine	Et_3N (5)	24	60
7	dioxane	Et_3N (5)	24	64
8	DMF	Et_3N (5)	24	94
9	acetonitrile	DBU (5)	24	0
10	acetonitrile	imidazole (5)	24	0
11	acetonitrile	pyridine (5)	24	1
12	acetonitrile	DIPEA[c] (5)	24	68
13	acetonitrile	TMEDA[d] (5)	24	80
14	pyridine	none	24	6
15	acetonitrile	DMAP (5)	24	71
16	acetonitrile	DMAP (5) + Et_3N(5)	24	3
17	acetonitrile	DMAP (0.25) + Et_3N(5)	24	63

[a] Reactions were carried out with acetic anhydride (2 equiv) at 40 °C. [**1**] = 0.125 mol/L. [b] 10 equiv of acetic anhydride was used. [c] Diisopropyethylamine. [d] *N*,*N*,*N*′,*N*′-Tetramethylethylenediamine.

SCHEME 4

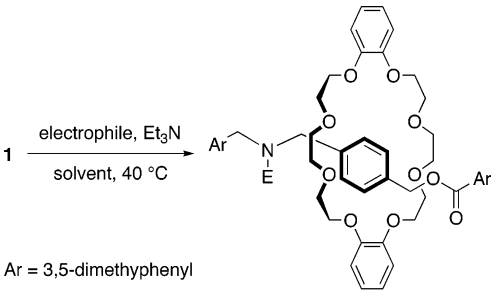

rotaxane	E
2	CH_3CO-
10	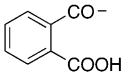
11	$ClCH_2CO-$
12	$BrCH_2CO-$
13	$PhCO-$
14	$PhCH_2OCO-$
15	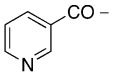
16	$PhNHCO-$
17	$EtNHCO-$

can explain the unusual effect of amines. The shape of the base can explain this unusual phenomenon. Thus, when a planar base with sp^2-hybridized nitrogen slides into the cleft between the wheel and the axle of the rotaxane, there is no space for the electrophile to access the ammonium group. On the other hand, the bulky base with sp^3-hybridized nitrogen opens the cleft to let the electrophile access the ammonium group. Although we were unable to obtain direct spectroscopic evidence for such behavior because of the low acidity of **1**, the characteristic behavior of DMAP as a base may support the above hypothesis. Since DMAP has both sp^2- and sp^3-hybridized nitrogens, DMAP alone worked effectively. However, when DMAP was added to the triethylamine-containing system, the yield of **2** greatly decreased as the amount of DMAP increased (runs 16 and 17). The negative catalytic effect of DMAP indicates that planar DMAP prevented proton abstraction by triethylamine.

Various electrophiles could be used for *N*-functionalization (Scheme 4). The results are summarized in Table 4. Less

TABLE 4. Effect of Electrophiles in the *N*-Acylation of 1[a]

run	electrophile (equiv)	rotaxane	solvent	base (equiv)	time/h	yield/%
1	phthalic anhydride (5)	**10**	DMF	Et_3N (15)	98	80
2	$(ClCH_2CO)_2O$ (10)	**11**	acetonitrile	Et_3N (5)	30	76
3	AcCl (2)	**2**	acetonitrile	Et_3N (5)	24	41
4	$BrCH_2COBr$ (10)	**12**	acetonitrile	Et_3N (5)	24	0
5	BzCl (2)	**13**	DMF	Et_3N (5)	98	1
6	BzCl (2)	**13**	acetonitrile	Et_3N (5)	98	70
7	BzCl (2)	**13**	THF	Et_3N (5)	98	85
8	CbzCl[b] (10)	**14**	DMF−toluene	Et_3N (5)	96	75
9	CbzCl[b] (10)	**14**	THF−toluene	Et_3N (5)	96	40
10	NicCl[c] (5)	**15**	pyridine	Et_3N (5)	48	94
11	PhNCO (2)	**16**	acetonitrile	Et_3N (5)	24	71
12	EtNCO (2)	**17**	acetonitrile	Et_3N (5)	100	36
13	EtNCO (2)	**17**	DMF	Et_3N (5)	48	66
14	PyBz[d] (10)	**13**	acetonitrile	Et_3N (5)	720	57

[a] Reactions were carried out at 40 °C. [**1**] = 0.125 mol/L. [b] Benzyloxycarbonyl chloride. [c] Nicotinoyl chloride hydrochloride. [d] *S*-2-pyridyl benzothioate.

electrophilic phthalic anhydride was successfully used to obtain 80% yield of **10** (run 1), although it took a long time (98 h). When chloroacetyl anhydride was used, the corresponding *N*-acylated [2]rotaxane **11** was obtained in 76% yield (run 2). The abstraction of the rather acidic α-hydrogen of chloroacetyl anhydride occurred simultaneously. Similarly, when acetyl chloride was used, **2** was obtained in a poor yield (41%) because of the formation of ketene under basic conditions (run 3). Further, no *N*-acylation product was obtained from bromoacetyl bromide (run 4). Meanwhile, since benzoyl chloride has no α-proton, benzoylated [2]rotaxane **13** was obtained in high yield (runs 5−7). In this case, THF was the best solvent. Benzyloxycarbonyl chloride and nicotinoyl chloride gave **14** and **15** in good yields, respectively (runs 8−10). Acylative neutralization was also possible with isocyanates (runs 11−13). Phenyl isocyanate gave a urea-type of rotaxane **16** in 71% yield. Although ethyl isocyanate also gave rotaxane **17**, the yield was rather low because the base-catalyzed trimerization of isocyanate took place simultaneously (runs 12 and 13). Further, acylation by the active ester sluggishly proceeded to give rotaxane **13** in 57% yield (run 14). The structures of all products were determined by elemental analyses in addition to spectral characterization.

^{1}H NMR Spectroscopic Analysis. The structure of rotaxanes and the location of wheel components were examined by ^{1}H NMR spectroscopy. The ^{1}H NMR spectrum of **1** in $CDCl_3$ is shown in Figure 1, where all signals were clearly assigned by the detailed NOE experiments. The numbering of the atoms indicated in Figure 1 is used throughout this paper. Among the two 3,5-dimethylphenyl groups, the signal of methyl protons on the benzyl-type phenyl ring (H2, 2.15 ppm) was observed at a field 0.21 ppm higher than that on the benzoyl-type phenyl ring (H10, 2.36 ppm). Since benzylic methyl proton signals in mesitylene and methyl 3,5-dimethylbenzoate were observed at 2.27 and 2.34 ppm, respectively, in $CDCl_3$, the upfield shift of H2 is characteristic of **1**. Since such a big upfield shift of the methyl group was not observed in the ^{1}H NMR spectrum of **6**, it can be attributed to the shielding effect of the benzene ring of the crown ether wheel component. While the wheel component was placed around the ammonium group in the crystal state (vide infra), the same localization occurred in the solution state. This was also confirmed by the NOE experiments. Thus, Hγ of the wheel showed NOEs with H2, H3, and H6 in 2.5%, 1.9%, and 3.8%, respectively. Since the wheel component is localized

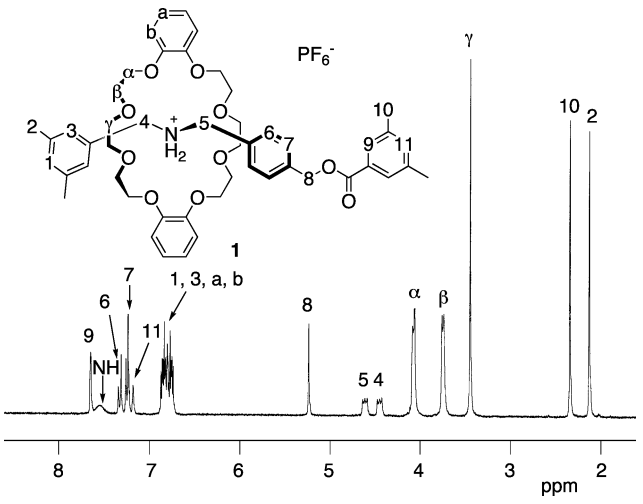

FIGURE 1. ^{1}H NMR spectrum (270 MHz, $CDCl_3$, 298 K) of **1**. All signals were assigned by the assistance of NOE experiments.

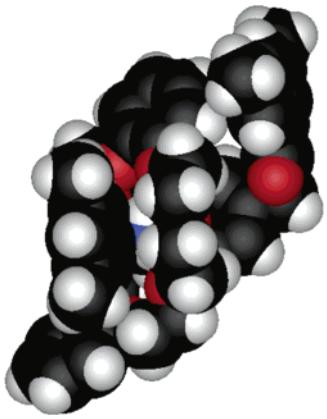

FIGURE 2. Space-filling model of **1** obtained by X-ray crystallographic analysis.

at the ammonium group, H2 is under the strong influence of the benzene ring of the wheel, while H10, which locates far from the wheel component, is out of the deshielding field (Figure 2).

The signals of the benzylic methylene protons attached to the ammonium group, H4 and H5, appeared at 4.48 and 4.64 ppm, respectively, as complex multiplet signals, while the corresponding proton signals of **3** were observed at 4.14 and 4.19 ppm, respectively, as singlets. The complex coupling and the downfield shift of H4 and H5 are characteristic of a rotaxane structure comprised of crown ether and secondary ammonium salt.[14] It is assumed that the CH···O hydrogen-bonding interaction of H4 and H5 with oxygen atoms in crown ether causes such downfield shift, as observed in similar systems.[15]

The coupling pattern observed in the H4 and H5 signals cannot be explained by first-order approximation. The decoupling of the ammonium protons at 7.56 ppm altered these

(14) Geores, N.; Loeb, S. J.; Tiburcio, J.; Wisner, J. A. *Org. Biomol. Chem.* **2004**, *2*, 2751−2756.

(15) (a) Ashton, P. R.; Chrystal, E. J. T.; Glink, P. T.; Menzer, S.; Schiavo, C.; Spencer, N.; Stoddart, J. F.; Tasker, P. A.; White, A. J. P.; Williams, D. J.; *Chem. Eur. J.* **1996**, *2*, 709−727. (b) Loeb, S. J.; Wisner, J. A. *Chem. Commun.* **2000**, 845−846. (c) Cantrill, S. J.; Pease, A. R.; Stoddart, J. F. *J. Chem. Soc., Dalton Trans.* **2000**, 3715−3734.

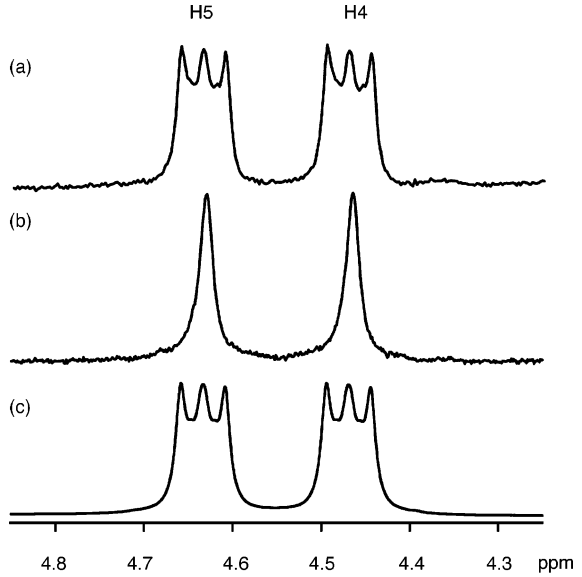

FIGURE 3. Partial ^{1}H NMR spectrum (270 MHz, $CDCl_3$, 298 K) of the (a) H4 and H5 signals of **1**, (b) same after the decoupling of the ammonium protons, and (c) simulated signals of H4 and H5 (parameters, see Table 5).

TABLE 5. ***J* Values for the Simulation of the Six Spin System $CH_2NH_2CH_2$ (H4A, H4B, NHA, NHB, H5A, and H5B) (Spectrum Is Shown in Figure 3c)**

		J value/Hz					
	half peak width/Hz	H4A	H4B	NHA	NHB	H5A	H5B
H4A	3.5						
H4B	3.5	10[a]					
NHA		10.5	3.2				
NHB		3.2	10.5	10[a]			
H5A	3.5	0[b]	0[b]	10.5	3.2		
H5B	3.5	0[b]	0[b]	3.2	10.5	10[a]	

[a] The three geminal coupling constants must be equal, although the value itself is within an error of about 2 Hz. [b] Although J_{H4-H5} can be larger than 0, it must be smaller than 0.3 Hz.

multiplets to slightly broader singlets, as shown in Figure 3b. This observation indicates that the *J* coupling between H4 or H5 and the ammonium protons caused the complex multiplets for H4 and H5. The NMR simulation of the six-spin system $CH_2NH_2CH_2$ (H4A, H4B, NHA, NHB, H5A, and H5B) was carried out to evaluate the *J* values. A set of *J* values was tuned to regenerate the observed ^{1}H NMR spectrum. It was revealed that all chemically equivalent protons (H4A and H4B, NHA and NHB, and H5A and H5B) are magnetically nonequivalent. One of the solutions is shown in Table 5, while the result of the simulation is shown in Figure 3c. H4 and H5 have rather large half peak widths (3.5 Hz) intrinsically, and very small (<0.3 Hz) *J* coupling between H4 and H5 is expected. To evaluate the reason for the rather large half-peak width value, T_2 measurements were carried out. The T_2's of H4 and H5 were 0.16 and 0.12 s, respectively, while that of H8 was 0.58 s. The unexpectedly short T_2 values of H4 and H5 indicate that the conformation of the spin system is highly restricted and that the free rotation of C4−N and C5−N bonds is not allowed. The set of *J* values (Table 5) and the magnetic nonequivalence of H4, NH, and H5 indicate that the system $ArCH_2NH_2CH_2Ar$ is fixed to an *s-trans* (zigzag) conformation. The fixation is obviously the result of the penetration of the ammonium axle into the crown ether wheel. It is reasonable to conclude the

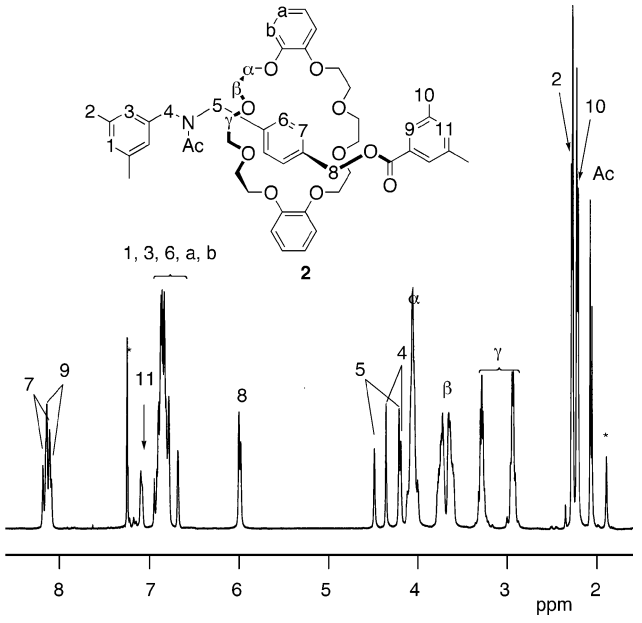

FIGURE 4. ^{1}H NMR spectrum (270 MHz, $CDCl_3$, 298 K) of **2**. All of the signals were assigned with the assistance of NOE experiments and the ^{1}H NMR spectrum of **2**-d_3. The asterisk denotes the signals of solvent and an impurity.

presence of a rotaxane-shaped complex when this type of multiplet coupling is observed in the ^{1}H NMR spectra of the ammonium salt−crown ether system.

The fixation of the $ArCH_2NH_2CH_2Ar$ system to a zigzag conformation indicates that the wheel component, crown ether, cannot move from the ammonium moiety. This is coincident with the low polarity of **1** as the ammonium salt on TLC. Since all ammonium protons form strong intramolecular hydrogen bonds, they do not interact with the silica gel stationary phase. Further, the difficulty in the *N*-acylation reaction obviously came from the fixation of crown ether on the ammonium group.

Figure 4 shows the ^{1}H NMR spectrum of *N*-acetylated rotaxane **2** in $CDCl_3$ at room temperature. All signals split into a couple of signals of ca. 7:13 integration ratio. Since the signals coalesced upon heating, the splitting came from the slow *s-cis*−*s-trans* conformation change of the amide group. All signals except for H4 and H5 were clearly assigned by the assistance of the NOE experiments. For the assignments of H4 and H5 signals, trideuterated **18**-d_3 and the corresponding **1**-d_3 and **2**-d_3 were prepared as shown in Scheme 5. Imine **19** was treated with lithium aluminum deuteride to give trideuterated amino alcohol **18**-d_3. **1**-d_3 was synthesized by triflic acid-catalyzed acylative end-capping.[9b] **2**-d_3 was prepared from **1**-d_3 as described above.

From the ^{1}H NMR spectrum of **1**-d_3, the assignment of H4, H5, and H8 signals of **1** was confirmed (Figure 1). Further, H4 and H5 signals of **2** were clearly assigned as shown in Figure 4 by the comparison of the ^{1}H NMR spectra of **2** and **2**-d_3.

In the ^{1}H NMR spectrum of **2**, the chemical shifts of methyl protons in the 3,5-dimethylphenyl groups of **2** were very different from those of **1**; i.e., H10 was observed at a higher field than H2, in opposite relationship with that of **1**. This is easily explained by assuming that while H2 in **1** was under the deshielding field of the benzene ring of the crown ether, H2 in **2** was out of the influence of the benzene ring. That is, the crown ether moved from being around the ammonium group to another

SCHEME 5

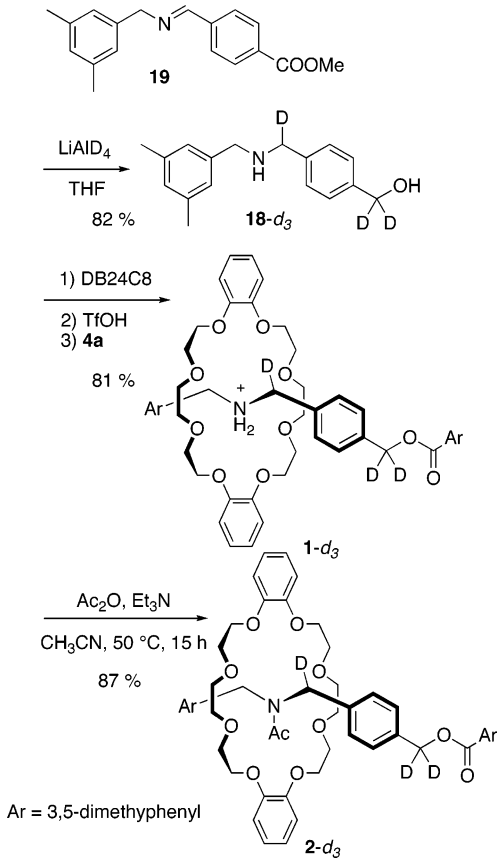

position on the axle. Instead of H2, H10 was included in the deshielding field. The most probable position of the crown ether on the axle can be estimated from the ^{1}H NMR spectra. Both H7 and H8 signals showed a remarkable downfield shift by the conversion from **1** to **2** (from 7.3 to 8.0 ppm for H7 and from 5.3 to 5.9 ppm for H8). It is very plausible that the anisotropic effect of oxygen atoms in the crown ether gave rise to these downfield shifts. Since such a downfield shift was not observed for H6, the crown ether should be positioned around H8, as confirmed by the NOE experiments. When Hβ in **2** was irradiated, NOE was observed at both H7 and H9, confirming that the crown ether was placed around H8. Since the signals of H7 and H9 were not distinct from each other, the respective NOE intensities could not be obtained. The average NOE intensity was 7.7% for H7 and H9.

The mobility of the crown ether on the axle can be estimated from the relaxation time by means of ^{1}H NMR techniques. The T_2 values observed for H4 and H5 of **2** were 0.25 and 0.25 s, respectively, which were longer than those of **1**, indicating that the mobility of H4 and H5 was enhanced by the conversion from **1** to **2**. On the other hand, the T_2 value of H8 in **2** was 0.18 s, which is much shorter than that in **1** (0.58 s). The mobility around H8 was highly restricted by the nearby crown ether, while H4 and H5 were free from the influence of the crown ether.

Another characteristic feature of the ^{1}H NMR spectrum of **2** is the splitting of the methylene signals of the crown ether. Hα splits only slightly, the splitting of Hβ is obvious, and Hγ splits largely. At first glance, the differentiation of the crown ether plane, i.e., amide-side and ester-side, seems to give rise to the splitting. In fact, Hβ and Hγ showed typical couplings of

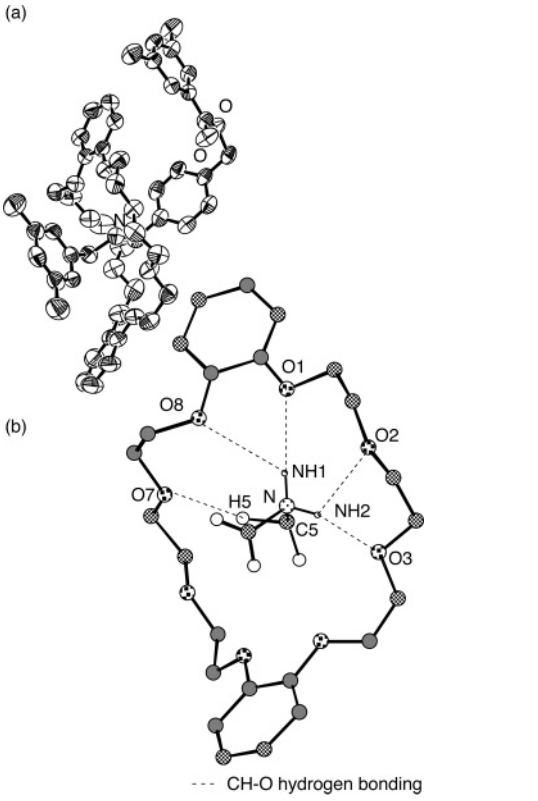

FIGURE 5. Crystal structure of **1** obtained by X-ray crystallographic analysis. (a) ORTEP drawing (50% probability ellipsoids) of **1**. Hydrogens, PF_6^- ion, and crystal water were omitted for clarity. (b) Part of a 3D model drawing of **1** to show the NH···O and CH···O hydrogen-bonding interactions. In accordance with the general numbering (Figure 1), hydrogens and carbons are numbered. The parameters of the intercomponent interactions are listed in Table 6.

AA′BB′ patterns. However, it is hard to understand why Hα, Hβ, and Hγ in **2** appear at a considerably higher magnetic field than in **1** and why the degree of splitting varies according to the position of the methylene groups. Although an upfield shift can be caused by the deshielding effect of the amide-carbonyl group introduced, the differences in chemical shifts were too great to be explained by the anisotropic effect of the carbonyl group. The origin of the splitting and the upfield shifts will be discussed following the X-ray crystallographic analyses.

X-ray Crystallographic Analysis. The structure of **1** obtained by X-ray crystallographic analysis is shown in Figure 5. Various types of hydrogen-bonding interactions were observed in the crystal structure of **1**. Both ammonium hydrogens were shown to have a network-like NH···O hydrogen-bonding interaction, which is the strongest interaction observed in **1**, with crown ether oxygen atoms. A rather weak CH···O hydrogen-bonding interaction was observed between the benzylic methylene protons attached to the ammonium group, H4 and H5 of the axle, and crown ether oxygen atoms, similarly to the previously reported systems.[16] The CH···O hydrogen-bonding caused the downfield shift of H4 and H5 signals in the ^{1}H NMR spectrum of **1** (Figure 1). As predicted from the ^{1}H NMR spectrum, the $ArCH_2NH_2CH_2Ar$ system of the axle has an all *s-trans* structure. It is thus obvious that the CH···O hydrogen-bonding interaction suppresses the free rotations of C4−N and

(16) Ashton, P. R.; Campbell, P. J.; Chrystal, E. J. T.; Glink, P. T.; Menzer, S.; Philp, D.; Spencer, N.; Stoddart, J. F.; Tasker, P. A.; Williams, D. J. *Angew. Chem., Int. Ed. Engl.* **1995**, *34*, 1865−1869.

TABLE 6. Parameter List in the Intercomponent Interactions

rotaxane	interaction atoms	distance/ Å	atoms or atom plane	angle/ deg
1	NH···O hydrogen bonding			
	N−O1	3.14		
	O1−NH1	2.28	N−NH1−O1	173.7
	N−O8	3.36		
	O8−NH1	2.80	N−NH1−O8	122.5
	N−O2	2.95		
	O2−NH2	2.44	N−NH2−O2	116.0
	N−O3	2.93		
	O3−NH2	2.05	N−NH2−O3	164.5
	CH···O hydrogen bonding			
	C5−O7	3.45		
	O7−H5	2.32	C5−H5−O7	157.0
2	CH···O hydrogen bonding			
	C6−O1	3.36		
	O1−H6	2.74	C6−H6−O1	121.9
	C6−O8	3.36		
	O8−H6	2.65	C6−H6−O8	129.3
	C7−O4	3.34		
	O4−H7	2.54	C7−H7−O4	142.5
	C7−O5	3.30		
	O5−H7	2.54	C7−H7−O5	137.9
	C8−O3	3.41		
	O3−H8A	2.68	C8−H8A−O3	130.8
	C8−O4	3.50		
	O4−H8A	2.78	C8−H8A−O4	130.0
	C8−O5	3.34		
	O5−H8B	2.77	C8−H8B−O5	120.2
	C8−O6	3.34		
	O6−H8B	2.64	C8−H8B−O6	135.0
	CH/π interaction			
	CγA-plane A	3.33		
	HγA-plane A	2.57	CγA-HγA−plane A	40.5
	CγB-plane A	3.36		
	HγB-plane A	2.65	CγB−HγB−plane A	43.8
15	CH···O hydrogen bonding			
	C7A−O1	3.38		
	O1−H7A	2.59	C7A−H7A−O1	140.5
	C7A−O8	3.49		
	O8−H7A	2.64	C7A−H7A−O8	149.2
	C7B−O4	3.28		
	O4−H7B	2.46	C7B−H7B−O4	136.5
	C7B−O5	3.36		
	O5−H7B	2.49	C7B−H7B−O5	142.3
	C8−O3	3.55		
	O3−H8A	2.83	C8−H8A−O3	125.7
	C8−O6	3.36		
	O6−H8B	2.55	C8−H8B−O6	145.5
	C9−O1	3.52		
	O1−H9	2.70	C9−H9−O1	152.4
	C9−O8	3.38		
	O8−H9	2.65	C9−H9−O8	139.6
	CH/π interaction			
	CγA-plane A	3.47		
	HγA-plane A	2.90	CγA−HγA−plane A	52.3
	CγB-plane A	3.53		
	HγB-plane A	2.83	CγB−HγB−plane A	51.9
20	CH···O hydrogen bonding			
	C1−O4	3.56		
	O4−H1A	2.59	C1−H1A−O4	156.3
	C1−O6	3.32		
	O6−H1B	2.40	C1−H1B−O6	155.7
	C2−O2	3.36		
	O2−H2A	2.31	C2−H2A−O2	169.0
	C2−O8	3.60		
	O2−H2B	2.71	C2−H2B−O8	157.8

C5−N bonds (Table 6). Therefore, the complex multiplet signals of H4 and H5 shown in Figure 3 are evidently the result of the conformational restrictions that are characteristic of the penetrating structure.

There is no $\pi-\pi$ interaction between the benzene rings involved in **1**. Considering that rotaxane **6** is obtained from dicyclohexano-crown ether in a high yield (Table 2), $\pi-\pi$ interaction is neither a significant driving force for pseudorotaxane formation nor the attractive intercomponent interaction of **1**.

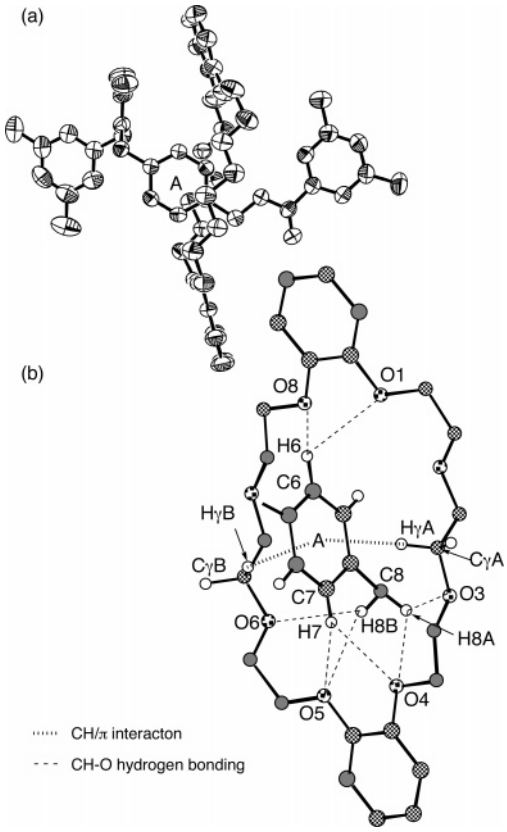

FIGURE 6. Crystal structure of **2** obtained by X-ray crystallographic analysis. (a) ORTEP drawing (50% probability ellipsoids) of **2**. Hydrogens were omitted for clarity. The 1,4-phenylene unit was shown as A. (b) Part of a 3D model drawing of **2** to show the CH···O hydrogen-bonding and CH/π interactions. In accordance with the general numbering (Figure 3), hydrogens and carbons are numbered. The parameters of the intercomponent interactions are listed in Table 6.

The crystal structure of *N*-acetylated rotaxane **2** is shown in Figure 6. As expected, *N*-acetylation shifts the crown ether from the ammonium group to the ester-end of the *p*-phenylene group. This coincides with the features of the ^{1}H NMR spectra. While the strong NH···O hydrogen-bonding interaction disappeared, many weak interactions appeared instead. Several CH···O hydrogen-bondings were observed between crown ether oxygen atoms and H6, H7, and H8. Thus, the downfield shifts of both H7 and H8 signals in **2** were attributed to the CH···O hydrogen-bonding interactions. Since CH···O hydrogen-bonding of H4 and H5 disappeared, both C4−N and C5−N bonds acquired free rotation allowing H4 and H5 to appear as singlet signals in the ^{1}H NMR spectrum of **2** (Figure 4).

A CH/π interaction[17] was clearly observed between some Hγs and the *p*-phenylene group. The CH/π interaction can nicely account for the large upfield shift and peak split of Hγ in the ^{1}H NMR spectrum (Figure 4), indicating a structural similarity between the solid and solution states of **2**. Although no clear CH/π interaction was observed for Hα and Hβ in the solid state,

(17) Nishio, M.; Hirota, M.; Umezawa, Y. *The CH/π Interaction*; Wiley-VCH: Toronto, 1998.

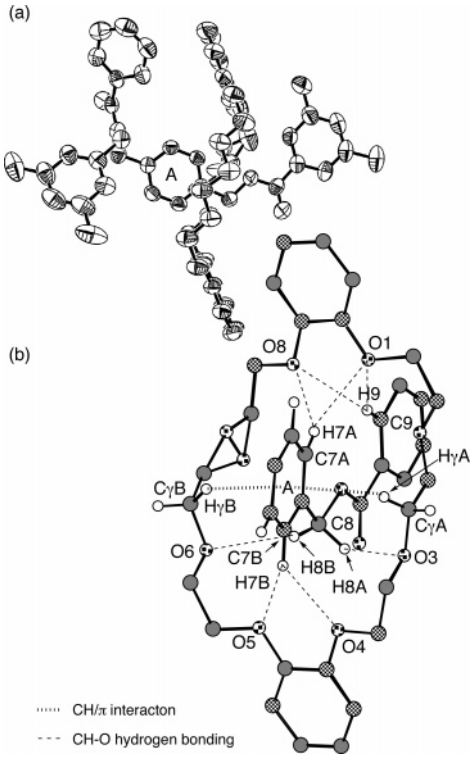

FIGURE 7. Crystal structure of **15** obtained by X-ray crystallographic analysis. (a) ORTEP drawing (50% probability ellipsoids) of **15**. Hydrogens were omitted for clarity. One oxygen of the crown ether is disordered. The 1,4-phenylene unit is shown as A. (b) Part of a 3D model drawing of **15** to show the CH···O hydrogen-bonding and CH/π interactions. One of the oxygens in the crown ether is disordered. In accordance with the general numbering (Figure 3), hydrogens and carbons are numbered. The parameters of the intercomponent interactions are listed in Table 6. One oxygen of the crown ether was disordered.

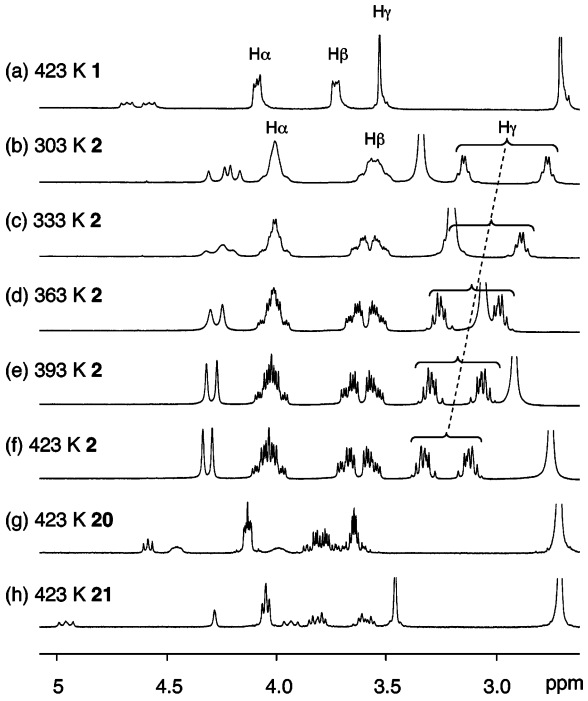

FIGURE 8. Partial ^{1}H NMR spectra (270 MHz) of **1**, **2**, **20**, and **21** in DMSO-d_6 at various temperatures.

their weaker peak split in the ^{1}H NMR spectrum is attributed to the weak CH/π interaction in solution due to the possible circumrotation of the wheel component around the axle component. Although the split of these methylene signals of the crown ether wheel is intrinsically caused by the face differentiation of the crown ether plane (vide infra), the CH/π interaction is supposed to amplify this difference to induce a larger split.

No $\pi-\pi$ interaction was observed between the benzene rings involved in **2** (Figure 6). Although several weak interactions were found in the crystal structure of **2** as well as **1**, the $\pi-\pi$interaction was assumed to be too weak to compete with other interactions.

To uncover the effect of the amide group on the structure of the *N*-acylated rotaxane, an X-ray crystal structure analysis of **15** was carried out (Figure 7). While the structure of **15** resembled that of **2**, the nicotinoyl group pushed the crown ether to the ester side more than the acetyl group. As a result,

TABLE 7. Crystallographic Data and Summary of Data Collection and Structure Refinement[a]

	1	2	15	20
formula	$C_{50}H_{64}F_6NO_{11}P$	$C_{52}H_{63}NO_{11}$	$C_{56}H_{64}N_2O_{11}$	$C_{46}H_{59}N_1O_{11}$
fw	1000.02	878.06	941.13	801.97
color, habit	colorless, block	colorless, block	colorless, block	colorless, block
crystal size (mm)	0.70x.0.20.x0.20	0.60 × 0.60 × 0.60	0.70x.0.30.x0.10	0.40 × 0.40 × 0.30
T (K)	293	296	296	296
cryst syst	triclinic	orthorhombic	orthorhombic	monoclinic
space grp	*P*-1 (No. 2)	*Pccn* (No. 56)	$P2_12_12_1$ (No. 19)	$P2_1/n$ (No. 14)
a, (Å)	11.8808(5)	18.9561(3)	14.9969(2)	14.6538(4)
b, (Å)	19.7939(7)	31.0160(5)	29.4294(4)	19.8519(5)
c, (Å)	11.3706(4)	16.5337(3)	11.8503(1)	15.3287(5)
α, deg	105.173(1)	90	90	90
β, deg	92.806(2)	90	90	93.445(1)
γ, deg	84.887(1)	90	90	90
V, (Å^3)	2569.6(2)	9720.9(3)	5230.1(1)	4451.1(2)
Z	2	8	4	4
d_{calcd}, (g·cm^{-3})	1.292	1.200	1.195	1.197
m (cm^{-1})	1.330	0.834	0.825	0.846
no. of meas	25652	11891	41587	40201
no. of obsd	7557	11046	6605	10120
no. of param	705	812	731	693
R [$I > 2\sigma(I)$][b]	0.092	0.045	0.045	0.065
R_w (all reflections)[c]	0.265	0.145	0.121	0.191
GOF on F^2	1.124	1.049	1.001	1.047

[a] Graphite-monochromated Mo Kα, refinement based on F^2. [b] $R = \Sigma\ ||F_o| - |F_c||/\Sigma|F_o|$. [c] $R_w = [\Sigma(w(F_o^2 - F_c^2)^2)/\Sigma w(F_o^2)^2]^{1/2}$.

SCHEME 6

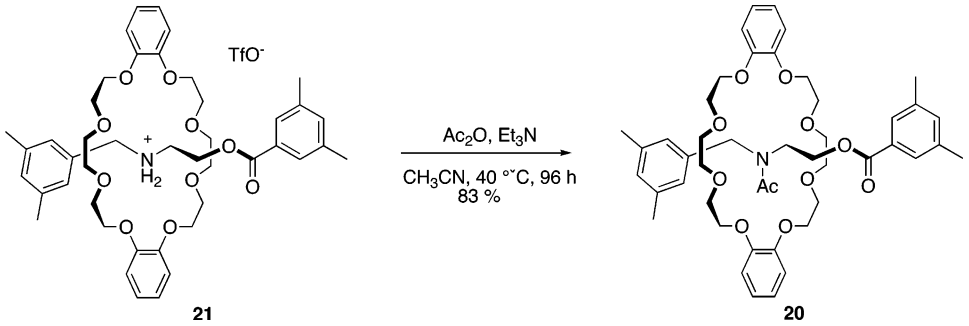

H6 lost its CH···O hydrogen-bonding, whereas H9 gained a CH···O hydrogen-bonding, as shown in Figure 7. A similar CH/π interaction to that of **2** was observed. Since CH···O hydrogen-bonding works nonselectively, it is reasonable to conclude that the CH/π interaction plays the main role in the conformation of *N*-acylated rotaxanes. The effect of the CH/π interaction in rotaxanes is discussed in detail in the following section.

CH/π Interaction in Rotaxane. Since the CH/π interaction is generally a weak one, the introduction of a small perturbation into the CH/π interaction-based interlocked system can induce a great conformational change. Therefore, the effect of the CH/π interaction working in a CH/π interaction-based rotaxane should be analyzed in detail in order to construct rotaxanes whose components can change their relative conformation sensitively.

Figure 8 shows the ^{1}H NMR spectra of **1** and **2** in DMSO-d_6 at various temperatures. In the case of **2**, Hγ shifted to a lower field as the temperature rose because the exothermic CH/π interaction weakened progressively at higher temperatures. Meanwhile, Hβ only slightly shifted at higher temperatures, and the shift of Hα was very small. These differences may be attributed to differences in the degree of contribution of the CH/π interaction.

The temperature-dependence of the chemical shift change of Hγ indicates that the CH/π interaction works even at 150 °C. To clarify the effect of the CH/π interaction, [2]rotaxane **20** was prepared from ethanolamine-based [2]rotaxane **21**, as shown in Scheme 6. There was no aromatic ring participating in the CH/π interaction of **20** and **21**. In the ^{1}H NMR spectra of **20** at 150 °C, the *s-cis*−*s-trans* conformation change of the amide groups was faster than the NMR time scale so that all signals coalesced and sharpened. A comparison of the ^{1}H NMR spectrum of **20** with that of **21** reveals that an upfield shift occurred for all methylene groups of the crown ether by ca. 0.1−0.2 ppm (Figure 8), presumably due to the influence of the anisotropic effect of the amide carbonyl. Therefore, the upfield shift larger than 0.2 ppm observed for **2** (0.23−0.29 ppm at 150 °C) can be attributed to the effect of the CH/π interaction working in the solution.

To reveal the structure of rotaxane without CH/π interaction, the X-ray crystal structure analysis of **20** was performed (Figure 9). CH···O hydrogen bonding was the only intercomponent interaction observable in **20**. Interestingly, the conformation of the crown ether wheel was quite different from that of **2** and **15**. It is very plausible that the CH/π interaction regulates the conformation of the crown ether wheel and that it is sufficiently strong to direct the structures of **2** and **15**.

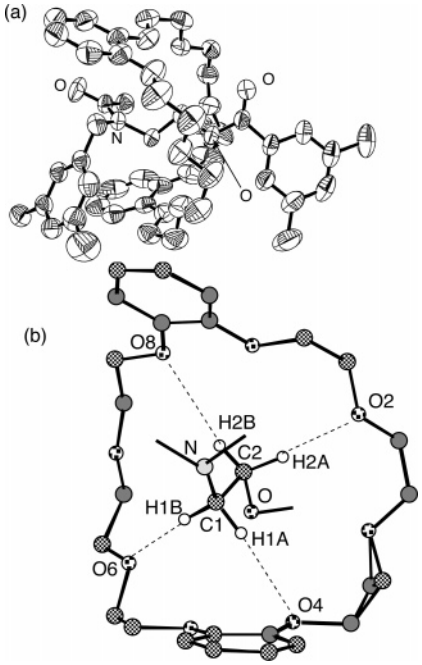

FIGURE 9. Crystal structure of **20** obtained by X-ray crystallographic analysis. (a) ORTEP drawing (50% probability ellipsoids) of **20**. Hydrogens were omitted for clarity. One carbon of the crown ether is disordered. (b) Part of a 3D model drawing of **2** to show the CH···O hydrogen-bonding interactions. The parameters of the intercomponent interactions are listed in Table 6. One carbon of the crown ether was disordered.

Conclusion

The present study demonstrated that selective *O*-acylation of ω-hydroxyalkyl *sec*-ammonium salt in the presence of a crown ether is one of the most effective and versatile methods to prepare rotaxanes. Thus, the acylative end-capping of the hydroxy group-terminated axle of pseudorotaxane using a combination of acid anhydride as acylating reagent and tributylphosphane as neutral catalyst gave rotaxanes quantitatively. Large-scale synthesis was easily performed without chromatographical purification. The subsequent *N*-acylation of the ammonium group in the presence of excess triethylamine and an acylation agent afforded the corresponding *N*-functionalized neutral rotaxane quantitatively. Because of the possible use of the various acylation agents and the quantitative yield, the present sequential acylation protocol provides a practical and useful method to prepare functionalized rotaxanes.

The strong hydrogen-bonding interaction between the crown ether and the ammonium group in the axle could be erased by *N*-acylative neutralization. Thereby, the CH/π interaction began

to work as the major intercomponent interaction instead of hydrogen bonding where the benzene ring was involved in the axle component. The CH/π interaction was too weak to obtain CH/π interaction-based interlocked compounds directly. However, these compounds could be prepared by the elimination of the strong intermolecular interaction initially utilized for the directed synthesis of interlocked compounds to reveal weak interactions such as CH···O hydrogen-bonding and CH/π interaction. These weak interactions are apparently hidden in rotaxanes with strong intercomponent interactions such as **1**. Since CH···O hydrogen bonding worked nonselectively, the CH/π interaction that selectively works on the benzene ring determined the conformation of rotaxane, e.g., the position of the wheel component on the axle component.

Rotaxane is considered as a basic form of molecular device in which the discontinuous and regulated change of the position of the wheel on the axle induced by the external stimulus plays an important role. If we want to activate or deactivate the rotaxane-based molecular switch with a faint stimulus, the rotaxane must consist of components with weak intercomponent interaction. Such a molecular switch may work faster. However, the preparation of a rotaxane using only weak interaction is very difficult. We demonstrated in this paper that the elimination of the strong intercomponent interaction preintroduced during the preparation of the rotaxane provides a weak interaction-based rotaxane which cannot be directly synthesized. The next objective would be the installation of an appropriate functional group that would handle the resulting weak interaction. We have demonstrated that the conformation of a ferrocene-containing rotaxane can be controlled by weak electrostatic interaction[18] and that intercomponent interaction can be controlled using the *N*-acylation protocol.[19] Also, the *N*-acylative neutralization protocol is useful to introduce functional groups such as the catalytically functional group.[20] Further functional rotaxanes with labile conformation are expected to be prepared using the sequential *O*- and *N*-acylation protocol.

Experimental Section

General Methods. ^{1}H and ^{13}C NMR spectra were recorded on JEOL GX270 (270 MHz) and GSX500 (500 MHz) spectrometers using tetramethylsilane as an internal standard. IR spectra were recorded on a JASCO FT/IR-230 spectrometer. FAB-MS analysis was made on a FINNIGAN MAT TSQ-70 instrument. Melting points were measured on a Yanako MP-3 instrument and were not corrected. X-ray diffractions were collected on a Rigaku R-AXIS RAPID-F graphite-monochromated Mo Kα radiation diffractometer with imaging plate, and the analysis was carried out with direct methods (SHELX-97[21] or SIR92) using Crystal Structure software. The program ORTEP3 was used to generate the X-ray structural diagrams.[22] Preparative GPC (eluent: chloroform) was performed using a Japan Analytical Industry LC-908 equipped with JAIGEL-1H and JAIGEL-2H columns. The simulation of ^{1}H NMR spectra was carried out with Adept gNMR ver. 4.0 software. Acetonitrile, toluene, and *N*,*N*-dimethylformamide were purified by distillation over calcium hydride before use. Ether, THF, and dioxane were distilled over benzophenone ketyl before use. 1,2-Dichloroethane and dichloromethane were used after treatment with phosphorus pentoxide followed by distillation over calcium hydride. Nicotinoyl chloride hydrochloride,[23] *S*-2-pyridyl benzoate,[24] and **21**[25] were prepared according to the literature. The preparations of other compounds are described in the Supporting Information. Other chemicals were reagent grade and used without further purification.

Preparation of Rotaxane by Tributylphosphine-Catalyzed Acylative End-Capping: General Procedure. A mixture of **3** and a slight excess of DB24C8 in dichloromethane (ca. 1 M) was stirred until a transparent solution was obtained. After the addition of a slight excess of **4a** and 5−10 mol % of tributylphosphine, the reaction mixture was allowed to stand for 3 h with continuous stirring. Water was added to the mixture to hydrolyze excess **4a**, and the resulting mixture was stirred for an additional 1 h. White precipitate formed was removed by filtration, and the filtrate was washed by 5% aqueous sodium carbonate and saturated aqueous ammonium hexafluorophosphate, dried with anhydrous magnesium sulfate, and evaporated. The crude product was purified by preparative GPC or recrystallization from ethyl acetate. The details are shown in Tables 1 and 2. Spectroscopic data of rotaxanes are listed in the Supporting Information.

***N*-Acylative Neutralization: General Procedure.** A solution of a rotaxane, an excess electrophile, and an excess triethylamine was stirred at 40−50 °C for the mentioned period. The reaction mixture was diluted with dichloromethane, washed with 1 M hydrochloric acid followed by saturated sodium carbonate solution, dried over anhydrous magnesium sulfate, and evaporated in vacuo. The crude product was purified by preparative GPC or silica gel column chromatography (eluent: dichloromethane−acetonitrile).

Acknowledgment. This work was financially supported by a Grant-in-Aid for Scientific Research on Priority Areas (A) (11133258 and 12020251) from the Ministry of Education, Culture, Sports, Science and Technology, Japan, and the Yazaki Memorial Foundation for Science and Technology.

Supporting Information Available: Experimental details and spectroscopic and analytical data for new compounds and crystallographic data for **1**, **2**, **15**, and **20** (CIF). This material is available free of charge via the Internet at http://pubs.acs.org.

JO0601563

(18) (a) Kihara, N.; Hashimoto, M.; Takata, T. *Org. Lett.* **2004**, *6*, 1693−1696. (b) Sandanayaka, A. S. D.; Sasabe, H.; Araki, Y.; Furusho, Y.; Ito, O.; Takata, T. *J. Phys. Chem. A* **2004**, *108*, 5145−5155. (c) Sandanayaka, A. S. D.; Watanabe, N.; Ikeshita, K.-I.; Araki, Y.; Kihara, N.; Furusho, Y.; Ito, O.; Takata, T. *J. Phys. Chem. B* **2005**, *109*, 2516−2525 (d) Kihara, N.; Motoda, S.; Yokozawa, T.; Takata, T. *Org. Lett.* **2005**, *7*, 1199−1202.

(19) Tachibana, Y.; Kihara, N.; Furusho, Y.; Takata, T. *Org. Lett*, **2004**, *6*, 4507.-4510

(20) Tachibana, Y.; Kihara, N.; Takata, T. *J. Am. Chem. Soc.* **2004**, *125*, 3438−3439

(21) Sheldrick, G. M. *Acta Crystallorg.* **1990**, *A46*, 467.

(22) Farrugia, L. J. *J. Appl. Crystallorg.* **1997**, *30*, 565

(23) *Organic Syntheses*; Wiley: New York, 1963; Collect. Vol. IV, p , 88.

(24) Rao, P. D.; Dhanalekshmi, S.; Littler, B. J.; Lindsey, J. S. *J. Org. Chem.* **2000**, *65*, 7323−7344.

(25) Rambacher, P.; Mäke, S. *Angew. Chem., Int. Ed.* **1968**, *7*, 465−466.